BRAIN
A JOURNAL OF NEUROLOGY

Post-acute delivery of erythropoietin induces stroke recovery by promoting perilesional tissue remodelling and contralesional pyramidal tract plasticity

Raluca Reitmeir,[1] Ertugrul Kilic,[2] Ülkan Kilic,[2] Marco Bacigaluppi,[3] Ayman ElAli,[1] Giuliana Salani,[3] Stefano Pluchino,[3] Max Gassmann[4] and Dirk M. Hermann[1]

1 Department of Neurology, University Hospital Essen, D-45122 Essen, Germany
2 Department of Physiology, Yeditepe University, TR-34755 Kayisdagi, Istanbul, Turkey
3 Neuroimmunology Unit and Institute of Experimental Neurology at DIBIT 2, San Raffaele Scientific Institute, I-20132 Milan, Italy
4 Department of Physiology and Zurich Centre for Integrative Physiology (ZIHP), University of Zurich, CH-8091 Zurich, Switzerland

Correspondence to: Prof. Dr Dirk M. Hermann,
Chair of Vascular Neurology,
Dementia and Ageing Disorders,
Department of Neurology,
University Hospital Essen,
Hufelandstr. 55,
D-45122 Essen, Germany
E-mail: dirk.hermann@uk-essen.de

The promotion of post-ischaemic motor recovery remains a major challenge in clinical neurology. Recently, plasticity-promoting effects have been described for the growth factor erythropoietin in animal models of neurodegenerative diseases. To elucidate erythropoietin's effects in the post-acute ischaemic brain, we examined how this growth factor influences functional neurological recovery, perilesional tissue remodelling and axonal sprouting of the corticorubral and corticobulbar tracts, when administered intra-cerebroventricularly starting 3 days after 30 min of middle cerebral artery occlusion. Erythropoietin administered at 10 IU/day (but not at 1 IU/day), increased grip strength of the contralesional paretic forelimb and improved motor coordination without influencing spontaneous locomotor activity and exploration behaviour. Neurological recovery by erythropoietin was associated with structural remodelling of ischaemic brain tissue, reflected by enhanced neuronal survival, increased angiogenesis and decreased reactive astrogliosis that resulted in reduced scar formation. Enhanced axonal sprouting from the ipsilesional pyramidal tract into the brainstem was observed in vehicle-treated ischaemic compared with non-ischaemic animals, as shown by injection of dextran amines into both motor cortices. Despite successful remodelling of the perilesional tissue, erythropoietin enhanced axonal sprouting of the contralesional, but not ipsilesional pyramidal tract at the level of the red and facial nuclei. Moreover, molecular biological and histochemical studies revealed broad anti-inflammatory effects of erythropoietin in both hemispheres together with expression changes of plasticity-related molecules that facilitated contralesional axonal growth. Our study establishes a plasticity-promoting effect of erythropoietin after stroke, indicating that erythropoietin acts via recruitment of contralesional rather than of ipsilesional pyramidal tract projections.

Introduction

Stroke remains the leading cause of serious motor disabilities in adults (Bonita *et al.*, 1994). Whereas initially hemiparesis affects 80–90% of patients, 45–60% still exhibit motor deficits in the post-acute stroke phase (Dobkin, 1996). Thus, neurological recovery is limited. Post-ischaemic endogenous responses of the CNS go in line with an enhanced responsiveness to rehabilitative (Biernaskie *et al.*, 2004) and plasticity-promoting (Papadopoulos *et al.*, 2002; Seymour *et al.*, 2005) treatments, opening a time window in which ontogenetic brain repair mechanisms may be reactivated successfully (Cramer and Chopp, 2000; Buchli and Schwab, 2005).

Stroke recovery is associated with reorganization of neuronal circuits both at the cortical and subcortical level. Latent networks are unmasked or strengthened, assuring the interaction between perilesional and distant brain areas. In the ischaemic boundary zone, a cascade of events including angiogenesis (Chen *et al.*, 2003), inhibition of astrogliosis (Li *et al.*, 2005) and anti-inflammation (Bacigaluppi *et al.*, 2009) contribute to the remodelling of brain tissue. In addition, a series of events set the stage for brain reorganization in the intact hemisphere, such as increased angiogenesis (Ding *et al.*, 2008) and axonal sprouting (Papadopoulos *et al.*, 2002; Wiessner *et al.*, 2003). Previous studies have examined ipsilesional and contralesional recovery processes independent of each other. There are no studies evaluating how both processes are coordinated.

Recruitment of contralesional brain areas correlate with a better recovery from stroke in animal studies (Papadopoulos *et al.*, 2002; Wiessner *et al.*, 2003). By administering anterograde tract tracers into the contralesional motor cortex, these authors suggested that contralateral projections may be recruited by plasticity-promoting therapies, underlining the relevance of contralesional reorganization in neurological recovery. However, models of permanent focal cerebral ischaemia were used in the latter studies, in which motor cortex tissue was destroyed. Brain plasticity ipsilateral to the stroke was not systematically assessed in these studies.

Evidence from positron emission tomography, functional magnetic resonance imaging, transcranial magnetic stimulation and magnetoencephalography studies has also supported the relevance of contralesional brain plasticity for human stroke recovery (Cramer *et al*, 1997; Musso *et al.*, 1999; Gerloff *et al.*, 2006; van der Zijden *et al.*, 2008). However, the implications of contralesional activation were difficult to interpret as activation patterns in humans are strongly influenced by severity and inhomogeneity of strokes. Whether the promotion of functional neurological recovery with growth factors influences contralesional reorganization processes was not described.

The identification of erythropoietin and its receptor in neurons, astrocytes and cerebral microvascular endothelial cells, and its sustained production in the hypoxic-ischaemic CNS (Marti *et al.*, 1996; Bernaudin *et al.*, 2000; Grimm *et al.*, 2005) has established erythropoietin as a potent survival-promoting factor that inhibits neuronal ischaemic injury (Tan *et al.*, 1992; Kilic *et al.*, 2005a; Li *et al.*, 2007) and prevents infarction (Siren *et al.*, 2001; Kilic *et al.*, 2005a; Li *et al.*, 2007) by modulating distinct cytosolic signalling pathways (Siren *et al.*, 2001; Kilic *et al.*, 2005a, b). In cell culture, erythropoietin also potently induced endothelial cell proliferation (Bernaudin *et al.*, 1999) and capillary tube formation (Wang *et al.*, 2004), thus also indicating a role in angiogenesis (Li *et al.*, 2007).

Because erythropoietin is already clinically used with minimal side effects (e.g. Hudson and Sameri, 2002), experimental studies rapidly led to clinical trials, in which the growth factor was acutely administered to stroke patients. In a first proof-of-principle study, erythropoietin significantly enhanced neurological outcome and reduced ischaemic injury, indicating that the growth factor is both safe and beneficial (Ehrenreich *et al.*, 2002). In a subsequent larger study including 522 patients, in which erythropoietin was infused intravenously after acute ischaemic stroke both in patients with (60%) and without (40%) thrombolysis, erythropoietin did not improve clinical outcome, but unexpectedly increased the risk of bleeding, brain oedema and thromboembolic events in thrombolyzed patients (Ehrenreich *et al.*, 2009). Explorative analysis in patients not receiving thrombolytics reproduced some of the earlier findings, indicating that erythropoietin alone may be efficacious (Ehrenreich *et al.*, 2009). Due to the expansion of the therapeutic window for intravenous thrombolysis to 4.5 h (Hacke *et al.*, 2008), acute neuroprotection studies with erythropoietin in patients not receiving thrombolytics may unfortunately be unfeasible in the near future.

In addition to its survival-promoting activities, erythropoietin exhibits plasticity-promoting actions in models of slowly progressive neurodegeneration. Erythropoietin increased ventral mesencephalic fibre outgrowth in a rodent model of Parkinson's disease (McLeod *et al.*, 2006) and enhanced axonal sprouting in a model of optic nerve transection (King *et al.*, 2007). Recently, erythropoietin was also shown to promote perilesional tissue remodelling in a rat model of focal cerebral ischaemia (Li *et al.*, 2009). Until now, it has remained unknown if and how the post-acute delivery of erythropoietin after stroke influences axonal plasticity processes. Here, we have investigated this issue, using a strategy of simultaneous analysis of pyramidal tract sprouting ipsi- and contralateral to the stroke in mice, which we combined with a detailed histochemical evaluation of perilesional brain remodelling, thus characterizing how endogenous brain responses are modulated by erythropoietin.

Materials and methods

Animal groups

Experiments were performed in accordance to National Institutes of Health Guidelines for the Care and Use of Laboratory Animals with local government approval (Bezirksregierung Düsseldorf, TSG966/08). Male C57Bl6/j mice (8–10 weeks; 23–25 g) were submitted to 30 min of left-sided middle cerebral artery occlusion (Kilic *et al.*, 2005a, 2006, 2008). At 72 h post-ischaemia, animals received implantations of mini osmotic pumps into the left lateral ventricle that were randomly filled with 0.9% NaCl (vehicle) or erythropoietin (1 or 10 IU/day diluted in 0.9% NaCl) and were left in place during the subsequent 4 weeks (Fig. 1).

In addition to animals undergoing middle cerebral artery occlusion, sham-operated animals were also studied, in which vehicle filled pumps were implanted as specified.

One set of mice was used for studies on functional neurological recovery and for analysis of axonal plasticity ($n = 10$ animals per group; Fig. 1A). For this purpose, mice received anterograde tract tracer injections (see below) in both frontal motor cortices 42 days after the stroke was induced (Fig. 1A). Ten days later, these animals were sacrificed (Fig. 1A).

Additional male C57Bl6/j mice were also subjected to 30 min middle cerebral artery occlusion using the same protocol, followed by implantation of intra-ventricular pumps filled with vehicle or erythropoietin (10 IU/day in 0.9% NaCl) 3 days later. These animals were sacrificed at Days 3, 14 and 30 [for reverse transcriptase–polymerase chain reaction (RT–PCR) studies] or at Days 14, 30 or 52 (for conventional histochemical studies, immunohistochemistry and western blots) after the stroke ($n = 4$ animals per group, survival time and series) (Fig. 1B and C). For RT–PCR studies, additional sham-operated mice ($n = 4$) and control mice submitted to 30 min middle cerebral artery occlusion without pump implantation ($n = 4$) were also investigated. The latter sham operated and untreated mice were sacrificed at 3 days post-surgery.

Induction of focal cerebral ischaemia

Animals were anaesthetized with 1% isoflurane (30% O_2, remainder N_2O). Rectal temperature was maintained between 36.5 and 37.0°C

using a feedback-controlled heating system. Cerebral blood flow was analysed by laser Doppler flow recordings. Focal cerebral ischaemia was induced using an intraluminal filament technique (Kilic *et al.*, 2008). A midline neck incision was made and the left common and external carotid arteries were isolated and ligated. A microvascular clip was temporarily placed on the internal carotid artery. A silicon resin-coated nylon monofilament was introduced through a small incision into the common carotid artery and advanced to the carotid bifurcation for middle cerebral artery occlusion. Reperfusion was initiated 30 min later by monofilament removal. Laser Doppler flow changes were monitored up to 30 min after reperfusion onset. In sham-operated animals, a surgical intervention was performed, in which the neck was opened and the common carotid artery was exposed, but left intact, while laser Doppler flow recordings were performed. After the surgery, wounds were carefully sutured, anaesthesia was discontinued and animals were returned to their cages. Animal drop-outs rarely occurred during and following 30 min middle cerebral artery occlusion ($<10\%$ of animals) and were related mostly to anaesthesia complications or surgical mistakes.

Intra-ventricular pump implantation

Three days after surgery animals were re-anaesthetized with 1% isoflurane (30% O_2, remainder N_2O) and cannulae (Brain infusion kit 3, Alzet, Cupertino, CA, USA) linked to mini osmotic pumps (Alzet 2004 or 1002; Alzet) filled with 0.9% NaCl or erythropoietin (NeoRecormon, Roche, Basel, Switzerland) (1 or 10 IU/day in 0.9% NaCl)
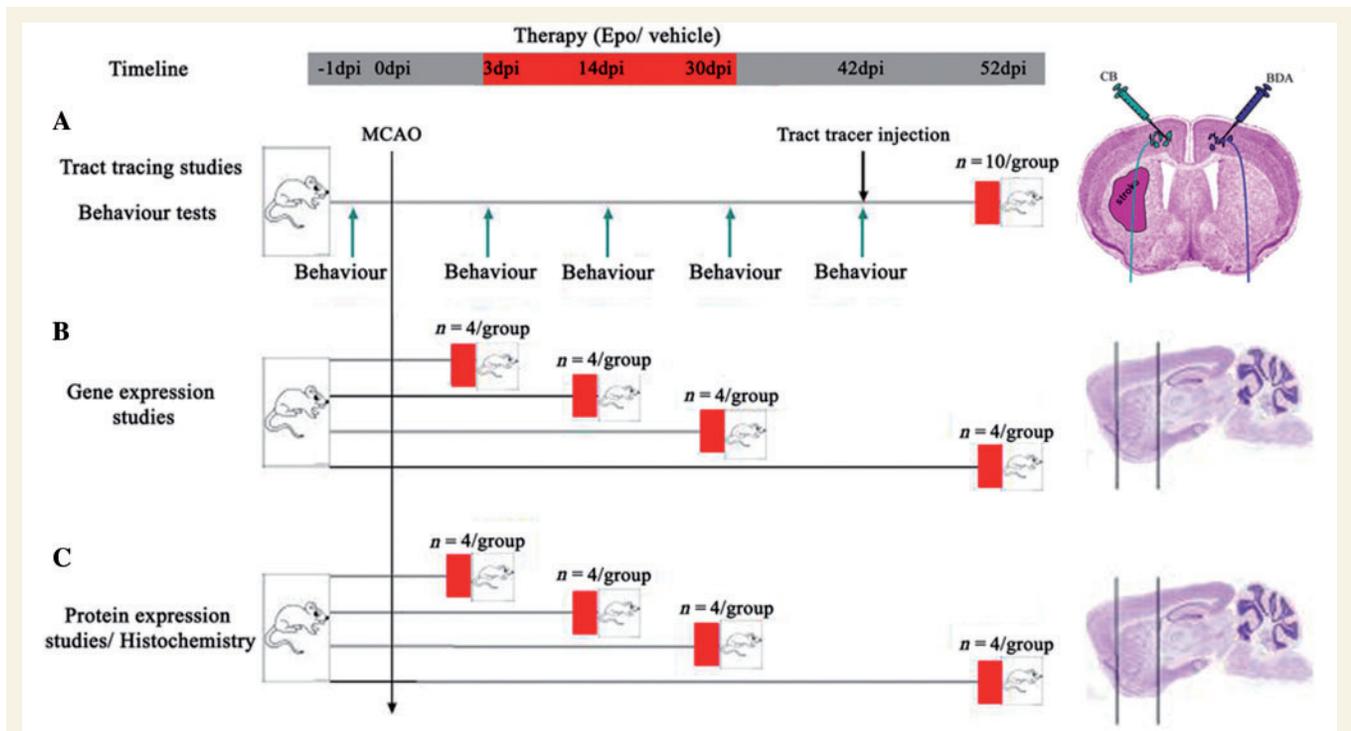

Figure 1 Experimental procedures and animal groups. Mice submitted to middle cerebral artery occlusion (MCAO) that were treated with erythropoietin (Epo) or vehicle from Days 3–30 post-ischaemia were used for (**A**) tract tracing studies and behavioural analysis, (**B**) gene expression studies (RT–PCR) and (**C**) protein expression studies (immunohistochemistry, western blots) and conventional histochemical analysis. Numbers of animals evaluated for each group and time points of animal sacrifice are also shown. (*Right*) The rostrocaudal level, from which brain sections and tissue samples were harvested. In addition to the animals shown in this scheme, additional sham-operated animals and ischaemic animals not receiving intra-ventricular pumps were generated as control groups in some of the studies, as outlined in the 'Materials and methods' section. BDA = biotinylated dextran amine; CB = cascade blue-labelled dextran amine; dpi = days post-ischaemia.

were implanted into the left-sided lateral ventricle through a burr hole (Kilic *et al.*, 2010). These pumps administered an infusion volume of 0.25 µl/h. The pumps were left in place until Day 30 post-ischaemia and then removed. Dropouts during pump implantation were also rare (<10% of animals) and occurred mostly as anaesthesia complications. Thus, such dropouts did not have significant effects on the results of this study. Following pump implantation, no intra-cerebral bleedings and no overt infections were noticed around the needle tracks. Two animals removed their pumps before Day 30 after ischaemia. These animals were not included in the data analysis.

Functional neurological tests

Functional neurological recovery was assessed using a battery of tests at baseline and on Days 3, 14 and 42 after middle cerebral artery occlusion.

Grip strength test

The grip strength test consists of a spring balance coupled with a Newton meter (Medio-Line Spring Scale, metric, 300 g, Pesola AG, Switzerland) that is attached to a triangular steel wire, which the animal instinctively grasps. When pulled by the tail, the animal exerts force on the steel wire (Kilic *et al.*, 2010). Grip strength was evaluated at the right paretic forepaw, the left non-paretic forepaw being wrapped with adhesive tape. Grip strength was evaluated five times in each test, for which mean values were calculated. From these data, percentage values (post-ischaemic versus pre-ischaemic) were computed. Pre-ischaemic and pretreatment results did not differ between groups.

RotaRod test

The RotaRod consists of a rotating drum with a speed accelerating from 6 to 40 rpm (Ugo Basile, model 47600, Comerio, Italy), to assess motor coordination skills (Kilic *et al.*, 2010). Maximum speed was reached after 245 s, and the time at which the animal dropped off the drum was evaluated (maximum testing time: 300 s). Measurements were performed five times and for all five measurements, mean values were computed, from which percentage values (post-ischaemic versus pre-ischaemic) were calculated. Pre-ischaemic and pretreatment data did not differ between groups.

Elevated O maze

The elevated O maze consists of a round 5.5 cm wide polyvinyl chloride runway with an outer diameter of 46 cm that was placed 40 cm above the floor and detected spontaneous locomotor behaviour and correlates of fear and anxiety (Kilic *et al.*, 2010). Two opposing 90° sectors were protected by 16 cm high inner and outer walls made of polyvinyl chloride (closed sectors). The remaining two 90° sectors were not protected by walls (open sectors). Animals were released in one of the closed sectors and observed for 10 min. The total number of zone entries—as correlate of motor activity—and the time spent in the unprotected sector—as correlate of exploration behaviour, fear and anxiety—were registered whenever the animal moved into a sector with all four paws. Assessments took place at baseline and at 2 and 6 weeks post-stroke.

Delivery of cascade blue-labelled dextran amine and biotinylated dextran amine

The anterograde tract tracer biotinylated dextran amine (BDA) has previously been used to evaluate pyramidal tract plasticity contralateral to the stroke in rats submitted to permanent focal cerebral ischaemia (Wiessner *et al.*, 2003). We here adopted this method to mice, administering two different tracers, cascade blue-labelled dextran amine (CB) and BDA in the motor cortex both ipsilateral (cascade blue) and contralateral (BDA) to the stroke. For this purpose, cranial burr holes were drilled 0.5 mm rostral and 2.5 mm lateral to the bregma, via which deposits of 10% cascade blue or 10% BDA (both 10 000 molecular weight; Molecular Probes, diluted in 0.01 M phosphate-buffered saline at pH 7.2) were placed into the motor cortex by means of microsyringe injections 6 weeks after middle cerebral artery occlusion. Therefore, a total volume of 2.1 µl of tracer was administered to each animal, injected in three equal deposits located rostrally, medially and caudally of the burr hole inside the motor cortex. The syringe was inserted into the brain at angles of 45°, 90° and 135° against the midline at a depth of 1.5 mm (Z'Graggen *et al.*, 1998). Tract tracer injections did not result in animal dropouts. No macroscopical bleedings and no overt infections were observed around the tracer deposits.

Ten days after the tracer injection, mice were transcardially perfused with 0.1 M phosphate-buffered saline pH 7.4 containing 100 000 IU heparin and 0.25% $NaNO_2$ followed by 4% paraformaldehyde in 0.1 M phosphate-buffered saline and 5% sucrose. Brains were removed and post-fixed overnight in 4% paraformaldehyde in 0.1 M phosphate-buffered saline and 5% sucrose and cryoprotected in increasing concentrations of sucrose (5, 10 and 30%) over 3 days. The tissue was then frozen with isopentane and cut into 20 and 40 µm thick coronal cryostat sections that were used for conventional and tract tracing histochemistry.

Immunohistological stainings at the level of ischaemic striatum

For conventional immunohistochemistry, four animals from each group were transcardially perfused with 0.9% NaCl at Days 14, 30 and 52 after the stroke. Brain tissue was frozen on dry ice and cut on a cryostat into 20 µm coronal sections (Kilic *et al.*, 2010). Brain sections from the level of the bregma (i.e. midstriatum) were fixed in 4% paraformaldehyde in 0.1 M phosphate-buffered saline, rinsed, pretreated for antigen retrieval with 0.01 M citrate buffer (pH 5.0), rinsed and immersed for 1 h in 0.1 M phosphate-buffered saline containing 0.3% Triton X-100 and 10% normal donkey serum. Brain sections were incubated overnight at 4°C with monoclonal mouse anti-NeuN (MAB377; Chemicon), monoclonal rat anti-CD31 (#557355; BD Biosciences), monoclonal mouse anti-glial fibrillary acidic protein (GFAP) Alexa Fluor 555 conjugated (#3656; Cell Signalling), monoclonal rat anti-CD45 antigen (#550539; BD Pharmingen) and polyclonal rabbit anti-ionized calcium binding adaptor protein (Iba-1) (Wako Chemicals, Neuss, Germany) antibodies (diluted 1:100 in 0.1 M phosphate-buffered saline) that were detected with Cy3 or Cy2 conjugated secondary antibodies (Jackson ImmunoResearch, Suffolk, UK). Sections were counterstained with 4′-6-diamidino-2-phenylindole (DAPI). In some experiments (CD45, Iba1) biotinylated secondary antibodies were used that were detected with avidin–biotin kit (Vector Laboratories, Burlingame, CA, USA) followed by 3,3′-diaminobenzidine (DAB) (#D4418, Sigma, Missouri, USA) staining. Sections were evaluated under a fluorescence microscope (Olympus BX 41) connected to a CCD camera (CC12; Olympus). Surviving neurons (NeuN^{+}), microvascular profiles (CD31^{+}), reactive astroglia (GFAP^{+}), leucocytes (CD45^{+}) and microglia (Iba1^{+}) were analysed in a blinded way by counting numbers of cells or profiles in six defined regions of interests per striatum measuring 62 500 µm², both ipsi- and contralateral to the stroke (Kilic *et al.*, 2005a, 2006). Two sections were processed for

each animal. Mean values were calculated for both sections for the whole striatum. With these data, neuronal survival, capillary density, astrogliosis, leucocyte infiltration and microglial activation were determined. In case of glial fibrillary acidic protein stainings, the overall area of scar tissue was outlined using the Soft Imaging Olympus Cell F Programme. Stereometric assessments of the degree of post-ischaemic atrophy of the striatum and corpus callosum were determined using modified Bielschowsky's silver stainings as previously described (Ding *et al.*, 2008).

Immunohistochemistry for cascade blue-labelled dextran amine and biotinylated dextran amine

Brain sections of animals that had transcardially been perfused with paraformaldehyde were rinsed three times for 10 min each in 50 mM Tris-buffered saline (pH 8.0) containing 0.5% Triton X-100. For detection of cascade blue-labelled dextran amine, sections were immersed overnight at 4°C with polyclonal rabbit anti-cascade blue antibody (A-5760; Molecular Probes, 1:100), in 50 mM Tris-buffered saline (pH 8.0) containing 0.5% Triton X-100, followed by incubation for 1 h at room temperature with a horseradish peroxidase-labelled secondary anti-rabbit antibody (1:1000). For detection of BDA, sections were incubated overnight with avidin–biotin–peroxidase complex (ABC Elite; Vector Laboratories, Burlingame, CA, USA). Stainings were revealed with 3,3′-diaminobenzidine (DAB) containing 0.4% ammonium sulphate and 0.004% H_2O_2.

Analysis of corticorubral and corticobulbar projections

The location of tracer deposits was checked at the levels of the needle tracks, thus ensuring that the motor cortex had indeed been injected in all animals. To account for variability in tracer uptake in different mice, we first evaluated the number of tracer-stained fibres in the corticospinal tract both at the level of the red nucleus and facial nucleus. For this purpose, two consecutive sections were analysed, counting the number of fibres crossing the sections in four regions of interest of 2865 μm^2 each that had been selected in the dorsolateral, ventrolateral, dorsomedial and ventromedial portion of the corticospinal tract. By measuring the total area of the corticospinal tract using the Cell Software image system (Olympus) connected to an Olympus BX42 microscope, we calculated the overall number of labelled pyramidal tract fibres, as described previously (Z'Graggen *et al.*, 1998).

Analysis of corticorubral projections

Corticorubral projections were evaluated at the level of the parvocellular red nucleus (bregma –3.0 to –3.5 mm). A 500 μm long intersection line was superimposed on the brain midline. Those fibres crossing into the contralateral hemisphere in the direction of the red nucleus were quantified. For each animal, the total number of fibres counted was normalized with the total number of labelled fibres in the corticospinal tract and multiplied by 100, resulting in percent values of fibres crossing the midline. For both tracers, two consecutive sections were analysed. For both sections, mean values of labelled fibres were determined.

Analysis of corticobulbar projections

Corticobulbar projections were assessed at the level of the facial nucleus (bregma –5.8 to –6.3 mm). Two 500 μm long intersection

lines were superimposed on the sections parallel to the midline, both representing tangents touching the most lateral extension of the pyramidal tract. Along both lines those fibres crossing in the direction of the contra- and ipsilateral facial nucleus were quantified. For each animal, the total number of fibres counted was normalized with the number of labelled fibres in the corticospinal tract and multiplied by 100, resulting in percent values of fibres originating from the pyramidal tract. For both tracers, two consecutive sections were evaluated and mean values of labelled fibres were calculated.

Gene expression analysis by reverse transcriptase–polymerase chain reaction

For gene expression studies, mice were sacrificed at three different time points, i.e. Days 3, 14 and 30 after stroke by transcardiac perfusion with cold sterile 0.1 M phosphate-buffered saline containing 0.01 M EDTA (ethylenediaminetetraacetic acid, pH 7.4). Brains were immediately removed and dissected on dry ice. Blocks of tissue were cut from 2 mm rostral to 2 mm caudal to the bregma. From these blocks, samples were collected from six regions of interest: the motor cortex, the striatum and the parietal cortex both ipsilateral and contralateral to the stroke. All regions were processed in RNA-later® RNA stabilization reagent (#76104; Qiagen, Hilden, Germany) and stored at −80° until RNA extraction. Brain tissue samples were homogenized and total RNA was isolated.

One microgram of complementary DNA synthesized from 2 μg of total RNA was used for RT–PCR using predesigned TaqMan low density arrays as previously described (Pluchino *et al.*, 2008). Briefly, for each TaqMan low density array, there were eight separate loading ports that distributed the complementary DNA into a total of 48 wells, for a total of 384 different wells per card. Each well contains a specific primer and probe, capable of detecting a single gene. In our study, we designed the gene cards for 46 different genes (Supplementary Table 1) together with two housekeeping genes, glyceraldehyde-3-phosphate dehydrogenase (GAPDH) and 18S ribosomal RNA. The last one is a mandatory control provided by the manufacturer. RT–PCR was processed with samples obtained from individual animals (avoiding pooling of the tissue) from each of the six regions of interest, each sample containing 10 μl complementary DNA (1 μg).

RT–PCR was performed using Applied Biosystems 7900HT Fast-Real-Time PCR System. Gene cards were analysed using the threshold cycle (CT) relative quantification method. Threshold cycle values were normalized for endogenous reference [ΔC_T = CT (target gene) − CT (GAPDH)] and compared with a calibrator using the $\Delta\Delta C_T$ formula [$\Delta\Delta C_T = \Delta C_T$ (sample) − ΔC_T (calibrator)]. In this study, we consistently used GAPDH as endogenous control. As a calibrator sample, we utilized a brain obtained from an untreated mouse of the same age, sex and strain. Data were presented using the logarithmic transformation of fold induction ratios between ischaemic vehicle- and non-ischaemic vehicle-treated mice (middle cerebral artery occlusion effect) and of ratios between ischaemic erythropoietin 10 IU and ischaemic vehicle-treated mice (erythropoietin effect).

Western blot analysis

For western blot analysis, we used mice transcardially perfused with 0.9% NaCl at Days 3, 14 and 30 after the stroke. From the brains, which had also been used for immunohistochemistry, tissue samples were harvested from the motor cortex ipsilateral and contralateral to the stroke, immediately adjacent to the level at which cryostat sections were taken (0–2 mm caudal to bregma). Tissue samples belonging to

the same group were pooled, homogenized, sonicated and treated with protease inhibitor cocktail and phosphatase inhibitor cocktail (Kilic *et al.*, 2010). In these samples, protein content was evaluated using the Bradford method (Kilic *et al.*, 2010). Equal amounts of protein were subjected to sodium dodecyl sulphate–polyacrylamide gel electrophoresis, followed by protein transfer onto a polyvinylidene fluoride membrane (Bio-Rad, Hercules, CA, USA). Membranes were blocked in 5% non-fat milk in 50 mM Tris-buffered saline containing 0.1% Tween for 1 h at room temperature, washed in Tris-buffered saline containing 0.1% Tween and incubated overnight with mouse monoclonal SPRR1A antibody (provided by Prof. S.M. Strittmatter, Yale University, CT, USA), diluted 1:1000 in Tris-buffered saline containing 0.1% Tween. On the second day the membranes were washed and further incubated in blocking solution with peroxidase-conjugated goat anti-mouse antibody (Santa Cruz Biotechnology, Santa Cruz, CA, USA) for 1 h at room temperature. Blots were revealed using a chemiluminescence kit according to the manufacturer's protocol. Protein loading was controlled by stripping the blots and reprobing with β-actin antibody. Protein abundance was evaluated by analysing the intensity of the SPRR1A band using the ImageJ program. Three different blots were analysed and mean values were calculated from the results obtained. The relative level of protein expression was normalized to signal intensities measured in corresponding contralateral tissue samples harvested Day 3 after the stroke.

Statistical analysis

Behavioural tests were analysed by means of two-way repeated measurement analysis of variance (ANOVA; treatment versus time) at three different time-points starting with Day 3 post-stroke, at the time of erythropoietin administration. For those tests in which significant treatment or treatment by time interaction effects were noticed (at 0.05 level), one-way ANOVA were carried out for each time point, using *post hoc* least significant differences tests. Tract tracing data were evaluated by one-way ANOVA. Histochemical data, gene and protein expression studies were analysed by two-way ANOVA (treatment versus time). Whenever a treatment effect or treatment by time interaction effect was present at the 0.05 level, two-tailed *t*-tests were performed for each time point.

Results

Post-acute delivery of erythropoietin improves post-ischaemic neurological recovery

To evaluate if erythropoietin influences neurological recovery in the post-acute stroke phase, mice submitted to 30 min left-sided middle cerebral artery occlusion were intra-cerebroventricularly treated with vehicle or erythropoietin (1 or 10 IU/day) starting at Day 3 post-ischaemia. Laser Doppler flow measurements and body weight did not show any differences between groups (Fig. 2A and B). In all groups, laser Doppler flow decreased to ~15–20% of baseline during middle cerebral artery occlusion, followed by a rapid restoration of blood flow after reperfusion (Fig. 2A). Except for a transient mild reduction in body weight at Day 3 post-ischaemia (<10%) that was similarly registered in all groups, no abnormalities in weight development were seen (Fig. 2B).

Neurological recovery was investigated by grip strength (Fig. 2C) and Rotarod (Fig. 2D) tests, which assess motor force of the paretic right forelimb and motor coordination. Significant reductions in motor force (Fig. 2C) and coordination skills (Fig. 2D) were noticed in animals submitted to 30 min middle cerebral artery occlusion. In vehicle-treated ischaemic animals and in animals receiving erythropoietin at the low dosage (1 IU/day), grip strength and RotaRod performance remained largely unchanged over the entire observation period of 42 days (Fig. 2C and D). Conversely, in animals treated with erythropoietin at the higher dosage (10 IU/day), progressive improvement of motor force and coordination was observed at Days 14 and 42 post-ischaemia (Fig. 2C and D). Elevated O maze tests did not detect any differences in spontaneous locomotor activity and exploration behaviour between groups (Fig. 2E and F).

Post-acute delivery of erythropoietin promotes perilesional tissue remodelling

In order to assess whether the post-acute delivery of erythropoietin influences the remodelling of ischaemic brain tissue, histochemical studies were performed. Immunohistochemical stainings for the neuronal marker NeuN revealed slowly progressive degeneration in the striatum of vehicle-treated ischaemic mice, reflected by a continuous decline of surviving neurons (Fig. 3A) and striatal atrophy (Fig. 3B) that developed between Days 14 and 52 post-ischaemia. Notably, erythropoietin delivered at the higher dosage (10 IU/day) significantly increased neuronal survival (Fig. 3A), at the same time preventing striatal shrinkage (Fig. 3B). The thickness of the corpus callosum was not changed by erythropoietin (Fig. 3C).

To define erythropoietin's impact on angiogenesis, an accompaniment of successful neurovascular remodelling (Hermann and Zechariah, 2009), immunohistochemical stainings for the endothelial marker CD31 were assessed. Focal cerebral ischaemia was followed by an increase in the density of CD31$^+$ striatal capillaries to ~200% of baseline in vehicle-treated ischaemic mice that persisted for as long as 30 days after middle cerebral artery occlusion (Fig. 3D). Erythropoietin further increased the capillary density, which remained elevated until the end of the experiments, i.e. at Day 52 post-ischaemia (Fig. 3D).

To evaluate how erythropoietin influences the astroglial responses to stroke, stainings for the astrocyte marker glial fibrillary acidic protein were analysed. In vehicle-treated ischaemic mice, focal cerebral ischaemia went along with reactive astrocytes that were dispersed throughout the middle cerebral artery territory and persisted over the observation period of 52 days post-ischaemia (Fig. 3E). During erythropoietin therapy, reactive astrogliosis was less pronounced (Fig. 3E). However, this glial-inhibitory effect disappeared after pump removal, i.e. at Day 52 post-ischaemia, when reactive astrogliosis returned to values similar to those of vehicle-treated ischaemic animals (Fig. 3E).

In the most lateral portion of the striatum, a localized scar characterized by densely packed GFAP$^+$ astrocytes developed after Day 30, more clearly distinguishable at Day 52 post-ischaemia in
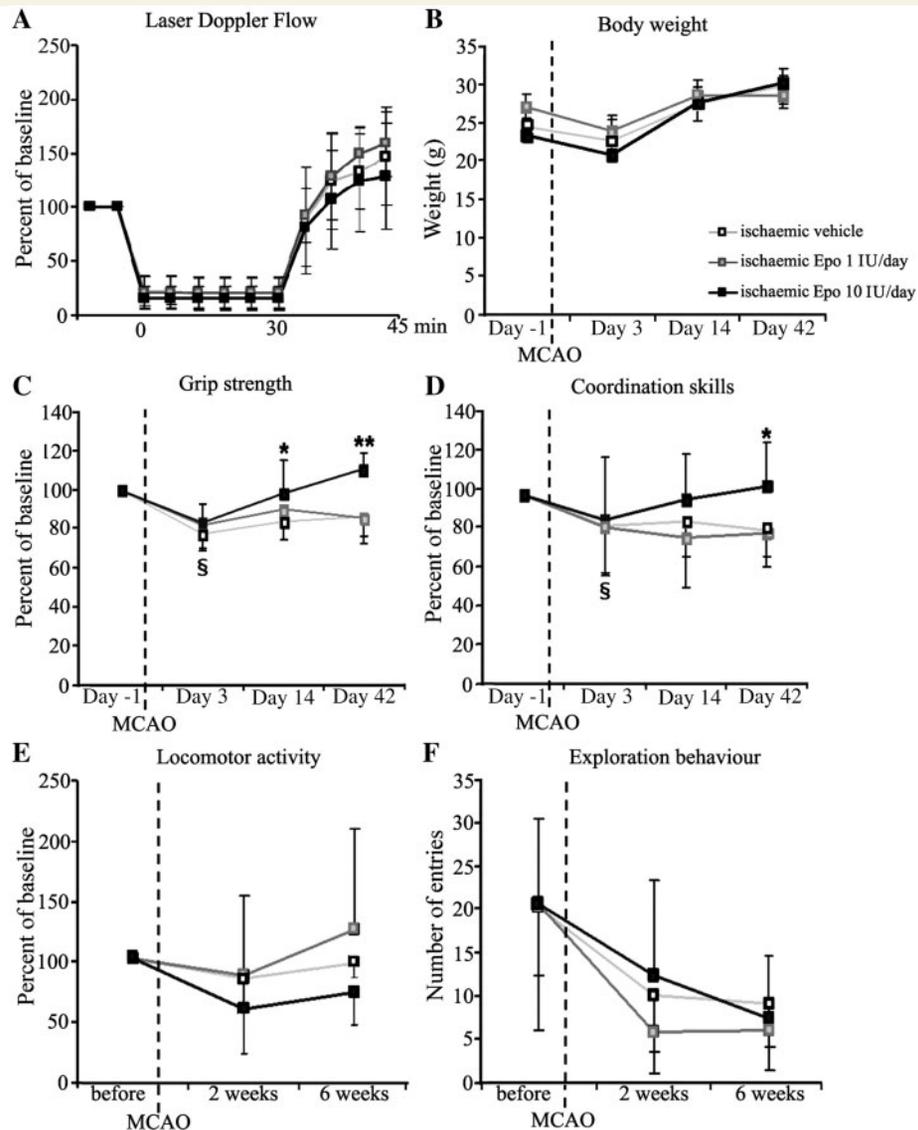
Figure 2 Delayed delivery of erythropoietin at 10 IU/day, but not 1 IU/day promotes post-ischaemic neurological recovery. (**A**) Laser Doppler flow recordings above the core of the middle cerebral artery territory, (**B**) body weight, (**C**) grip strength of the lesion-contralateral right paretic forepaw, (**D**) coordination skills evaluated by RotaRod tests, (**E**) locomotor activity and (**F**) exploration behaviour, assessed as number of total zone entries and time in open sectors in elevated O maze tests, are shown. Note that motor force (**C**) and coordination skills (**D**), which were compromised by the stroke, do not exhibit any major improvements over time in vehicle-treated mice and mice receiving erythropoietin at a dosage of 1 IU/kg, but progressively improve over Days 14–42 in animals treated with erythropoietin at a 10 IU/kg dosage. Spontaneous locomotor activity (**E**) and exploration behaviour (**F**) are not influenced by erythropoietin. Laser Doppler flow recordings (**A**) and body weight (**B**) do not differ between groups. Data are mean values ±SD. Data were analysed by two-way repeated measures ANOVA, followed by one-way ANOVA/least significant differences tests for each timepoint. $^{§}P < 0.05$ compared with pre-ischaemic baseline; $*P < 0.05$/$**P < 0.01$ compared with vehicle-treated ischaemic mice. Epo = erythropoietin; MCAO = middle cerebral artery occlusion.

vehicle-treated mice (Fig. 3F). Erythropoietin also reduced the size of this scar (Fig. 3F).

Analysis of lesion-remote plasticity using anterograde tract-tracers

Since the pyramidal tract crosses the middle cerebral artery territory, which was affected by ischaemia, we aimed to understand how erythropoietin influences pyramidal tract degeneration and plasticity both ipsilateral and contralateral to the stroke. To this end, we administered two dextran conjugates, cascade blue-labelled dextran amine and BDA, into both motor cortices. The location of injection sites revealed no relevant differences between groups. In all mice, the injection sites covered the more caudal forelimb area and rostral hindlimb area of the primary motor cortex without relevant spreading of tracer deposits into subcortical structures.
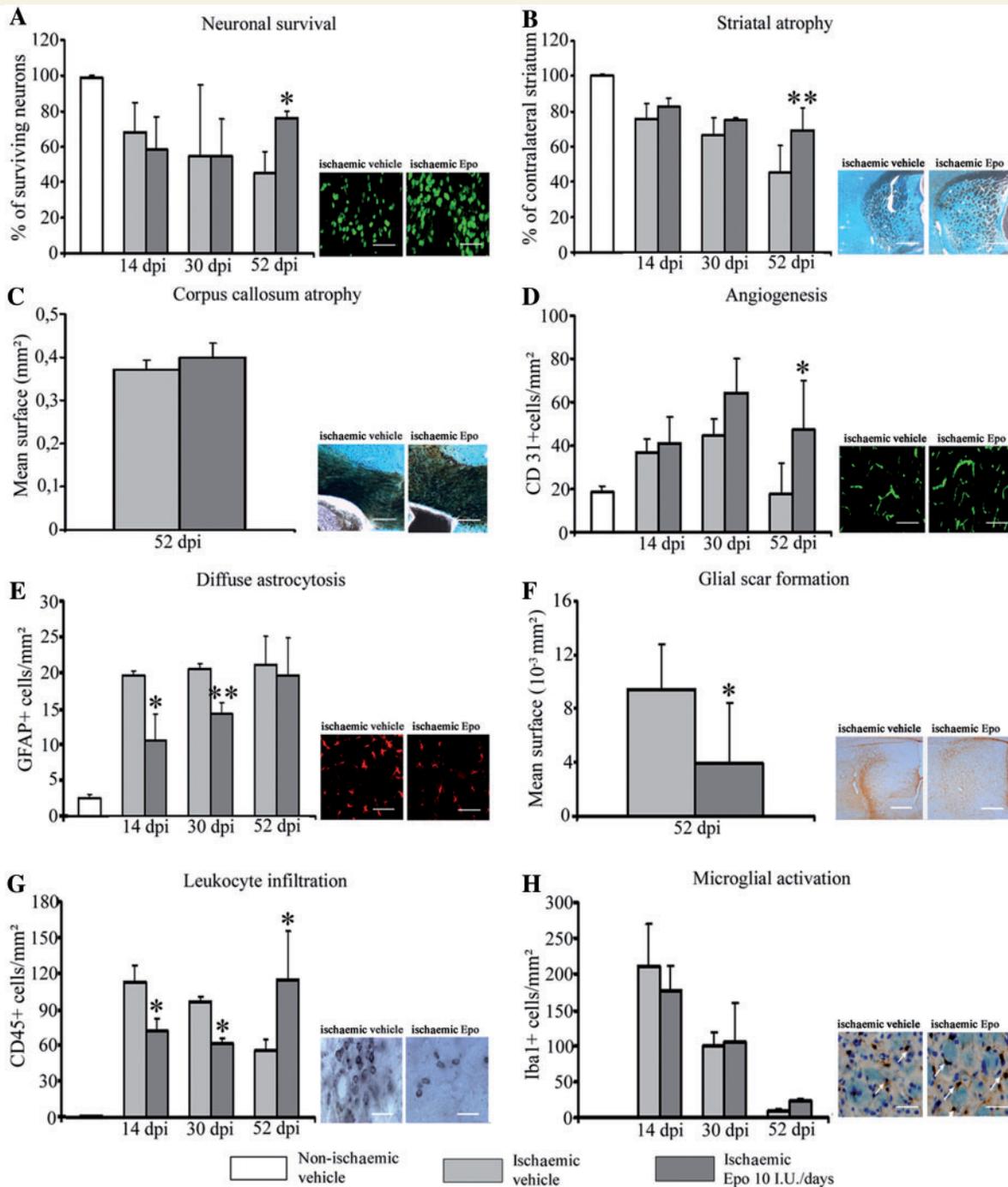
Figure 3 Erythropoietin (Epo) promotes peri-lesional tissue remodelling and exerts anti-inflammatory actions. (**A**) Surviving neurons in ischaemic striatum evaluated by NeuN immunohistochemistry, (**B**) striatal atrophy and (**C**) corpus callosum atrophy examined by Bielschowsky's stainings, (**D**) angiogenesis assessed by CD31 immunohistochemistry, (**E**) diffuse astrocytosis at various time points and (**F**) circumscribed scar formation in the most lateral striatum at Day 52 post-ischaemia revealed by glial fibrillary acidic protein (GFAP) immunohistochemistry. (**G**) Leucocyte infiltration and (**H**) microglial activation analysed by CD45 and Iba1 immunohistochemistry. Note that erythropoietin increases neuronal survival at Day 52 post-ischaemia (**A**), diminishes progressive brain atrophy (**B**) without influencing corpus callosum thickness (**C**), promotes angiogenesis (**D**), reduces diffuse astrocytosis (**E**) and glial scar formation (**F**) and inhibits leucocyte infiltration (**G**), without affecting microglial activation (**H**). Photomicrographs are also shown that were taken at Day 52 post-ischaemia (**A–D** and **F**) or Day 14 post-ischaemia (**E–H**). Data are mean values ±SD. Data were analysed by two-way ANOVA followed by two-tailed t-tests for individual time points. *$P < 0.05$/**$P < 0.01$ compared with vehicle-treated ischaemic mice. Bar = 200 μm (**B** and **F**); 50 μm (**C**); 20 μm (**A**, **D**, **E**, **G** and **H**).

To analyse whether erythropoietin influenced the survival of corticospinal tract fibres distant to the stroke lesion, we counted cascade blue-labelled dextran amine-labelled fibres in the cerebral peduncle both at the level of the red nucleus and facial nucleus. This quantification did not reveal any differences between vehicle- and erythropoietin-treated mice (red nucleus level: $44\,453 \pm 9944$ versus $44\,629 \pm 5509$ fibres/facial nucleus level: $19\,188 \pm 7383$ versus $19\,943 \pm 1592$ fibres, respectively), thus indicating that erythropoietin did not influence the survival of descending pyramidal tract axons. Similar to cascade blue-labelled fibres in the ipsilesional pyramidal tract, BDA-labelled fibres in the contralesional corticospinal tract did not differ between vehicle- and erythropoietin-treated mice. Similar to the total number of fibres, the overall size of the pyramidal tract, analysed on coronal sections at the bulbar level, was not changed by erythropoietin, either ipsilesional (0.06 ± 0.02 versus $0.07 \pm 0.03\,mm^2$), or contralesional (0.07 ± 0.01 versus $0.06 \pm 0.02\,mm^2$) to the stroke. As such, the corticospinal system was not affected by secondary degeneration.

Erythropoietin promotes contralesional, but not ipsilesional corticorubral plasticity

Cascade blue-labelled and BDA-stained fibres originating from the cerebral peduncle converted dorsomedially at mesencephalic levels, terminating as previously described (Z'Graggen *et al.*, 1998; Brown, 2007) in the parvocellular part of the ipsilateral red nucleus. At this level, we quantified the number of fibres crossing the midline towards the contralesional red nucleus. Our results revealed a moderate (though not significant) increase of the percentage of cascade blue-labelled midline crossing fibres derived from the ipsilesional corticospinal tract upon middle cerebral artery occlusion. On the other hand, the percentage of BDA-labelled midline crossing fibres originating from the contralesional corticospinal tract remained unchanged (Fig. 4). Importantly, erythropoietin significantly promoted the outgrowth of midline crossing fibres from the contralesional corticospinal tract, without influencing the plasticity of ipsilesional corticospinal tract fibres (Fig. 4).

Erythropoietin enhances contralesional, but not ipsilesional corticobulbar plasticity

At the midpontine level, two fibre bundles originating from the corticospinal tract innervate the ipsilesional and contralesional facial nucleus. At this level, we counted the fibres leaving the corticospinal tract in the direction of both facial nuclei, evaluating fibres crossing two intersection lines. Our data showed that focal cerebral ischaemia significantly increased the density of fibres originating from the cascade blue-labelled ipsilesional corticospinal tract innervating the ipsilesional facial nucleus, without affecting the density of fibres derived from the BDA-labelled contralesional corticospinal tract (Fig. 5). Erythropoietin significantly increased the sprouting of BDA-labelled contralesional corticospinal tract

axons to the contralesional facial nucleus, at the same time mildly but non-significantly ($P = 0.07$) reducing facial nucleus projections derived from the cascade blue-labelled ipsilesional corticospinal tract (Fig. 5).

Post-ischaemic remodelling by erythropoietin involves anti-inflammatory effects

To elucidate the mechanisms underlying erythropoietin's restorative actions, we performed semi-quantitative RT–PCR-based gene expression profiling, investigating a series of acute and chronic inflammation markers in the striatum, motor cortex and parietal cortex of both hemispheres (for complete list see Supplementary Table 1). As expected, stroke robustly increased several inflammation markers in the ischaemic hemisphere, among which there are interleukin (IL)-1β, tumour necrosis factor (TNF)-α, leukaemia-inhibitory factor (LIF), transforming growth factor (TGF)-β, IL-6, glial fibrillary acidic protein and inducible nitric oxide synthase (Fig. 6). Erythropoietin significantly reduced all these messenger RNAs in the ipsilesional, and to a lesser extent in the contralesional brain hemisphere (Fig. 6).

To further explore the immune changes induced by erythropoietin, we performed a scatter plot analysis, in which we correlated fold induction values from ischaemic and non-ischaemic regions for all inflammatory genes both at Days 14 and 30 post-ischaemia (Supplementary Fig. 1). Regression studies showed that the slope of the curve correlating fold induction values from erythropoietin treated with vehicle-treated animals was <1 in both hemispheres (between 0.37 and 0.6; Supplementary Fig. 1), further supporting the observation that erythropoietin exerts anti-inflammatory actions both ipsilaterally and contralaterally to ischaemic stroke.

In order to identify immune cells involved for the anti-inflammatory action of erythropoietin, immunostainings for the leucocyte marker CD45 and microglia marker Iba1 were performed. Erythropoietin significantly reduced the brain infiltration of CD45^{+} leucocytes (Fig. 3G), but not the presence of Iba1^{+} microglia (Fig. 3H) in the ischaemic striatum. In the contralesional hemisphere, neither Iba1^{+} microglia nor CD45^{+} leucocytes were seen. These data indicate that attenuation of leucocyte recruitment, besides reduced reactive astrogliosis, may contribute to erythropoietin's anti-inflammatory actions.

Modulation of pro-plasticity and anti-plasticity markers by erythropoietin

To better understand how erythropoietin influences brain plasticity both ipsilateral and contralateral to the stroke, additional RT–PCR studies were performed, using plasticity-promoting and -inhibitory genes that were previously described to be induced in the first days to weeks after stroke (Carmichael and Li, 2006; Supplementary Table 1). Induction of ischaemia was accompanied by a robust upregulation of the messenger RNAs of the pro-plasticity genes small proline-rich protein (*SPRR*)1, insulin-like growth factor (*IGF*)-1, brain-derived neurotrophic factor (*BDNF*),
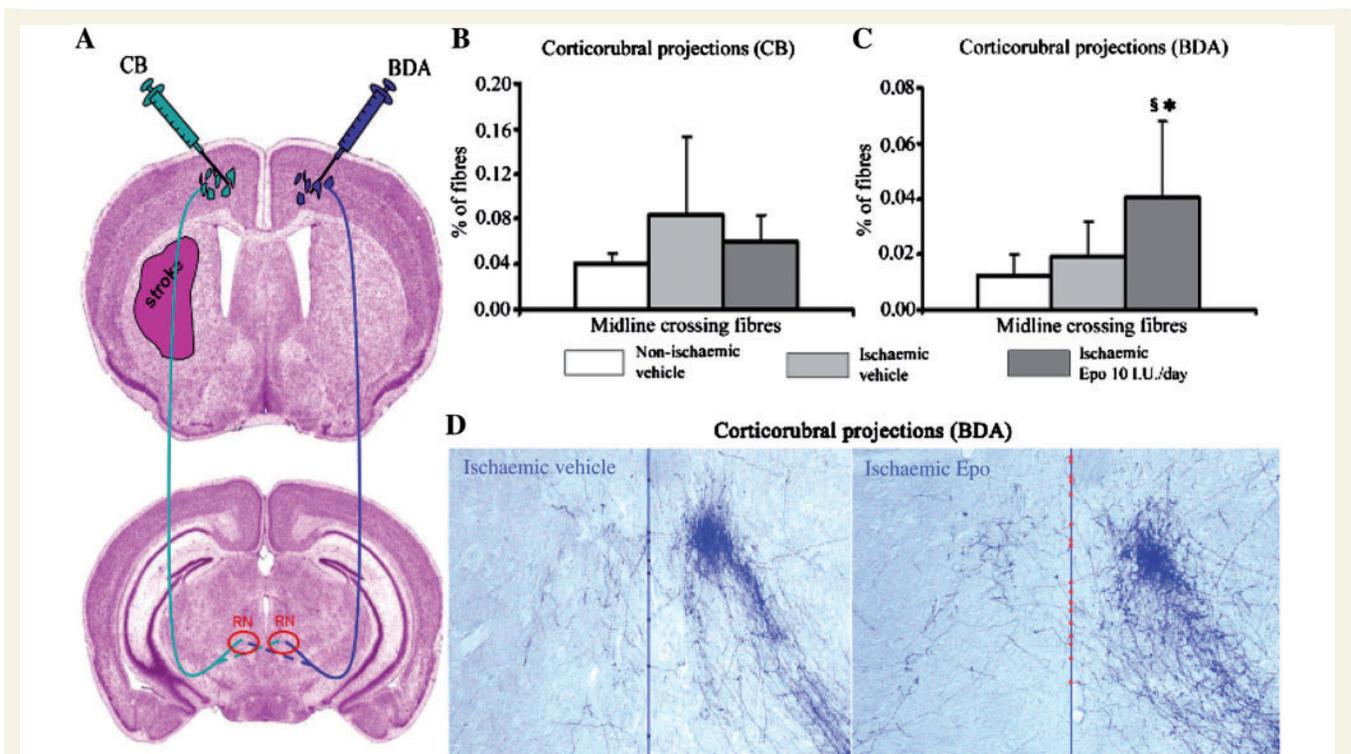
Figure 4 Erythropoietin (Epo) promotes contralesional, but not ipsilesional corticorubral plasticity. Tract tracing analysis of corticorubral projections ipsilateral and contralateral to the stroke in mice receiving cascade blue (CB) and biotinylated dextran amine (BDA) injections into the lesion-sided and contralesional motor cortex (for placement of tracer injections see (**A**). Percent of midline crossing fibres to (**B**) the contralesional red nucleus (RN) traced by cascade blue and (**C**) the ipsilesional, denervated red nucleus traced by BDA. Note that the percentage of midline crossing fibres after ipsilesional cascade blue injection moderately, but not significantly increases in response to stroke (**B**). Interestingly, erythropoietin (Epo) does not further elevate the percentage of midline-crossing fibres of the ipsilesional pyramidal tract (**B**), but increases contralesional pyramidal tract sprouting across the midline resulting in fibre outgrowth towards the denervated lesion-sided red nucleus (**C**). (**D**) Microphotographs of representative ischaemic vehicle- and erythropoietin-treated mice illustrating BDA traced corticorubral fibres intersecting the midline (superimposed in blue) in between both red nucleus. Note that the denervated (*left*) red nucleus receives more BDA traced fibres after erythropoietin than after vehicle delivery (midline-intersecting fibres labelled with dots). Data are means ±SD. Data were analysed by one-way ANOVA followed by least significant differences tests. $^{\S}P < 0.05$ compared with vehicle-treated non-ischaemic mice. $^{*}P < 0.05$ compared with vehicle-treated ischaemic mice.

vascular endothelial growth factor receptor-2 (*KDR*) and myristoylated alanine-rich C-kinase substrate (*MARCKS*) in the ischaemic but not the contralesional hemisphere between Days 3 and 30 post-ischaemia (Fig. 7). On the other hand, no comparably unequivocal pattern in the regulation of anti-plasticity messenger RNAs was observed (Fig. 7). Whereas erythropoietin diminished the expression of different pro-plasticity genes (i.e. *SPRR1*, *IGF-1* and *KDR*) in the ischaemic hemisphere at Day 14, but not Day 30 post-ischaemia, erythropoietin downregulated the anti-plasticity messenger RNAs neurocan and ephrin B1 and upregulated the pro-plasticity SPRR1 messenger RNA in the non-ischaemic hemisphere at Days 14 and 30 post-ischaemia (Fig. 7).

To further explore plasticity-modulating actions of erythropoietin in the stroke brain, we correlated fold induction values of erythropoietin- and vehicle-treated animals in scatter plots (Supplementary Figs 2 and 3). Regression studies revealed that the slope of the curve correlating fold induction values from erythropoietin- with vehicle-treated animals was <1 for pro-plasticity and anti-plasticity messenger RNAs in both hemispheres

at Day 14 post-ischaemia (between 0.50 and 0.79; Supplementary Figs 2 and 3). This slope remained low for anti-plasticity genes at Day 30 post-ischaemia (0.52–0.70), whereas the slope of pro-plasticity genes increased at the same time point contralateral to the stroke (to 1.18). These observations support our finding of a plasticity-promoting effect of erythropoietin in the contralesional hemisphere at Day 30 post-ischaemia.

To evaluate whether the expression of plasticity-related messenger RNAs also translates into proteins, we prepared western blots for the pro-plasticity protein SPRR1A using tissue samples obtained from the motor cortex. These blots revealed that, while SPRR1A expression was low in the contralesional motor cortex both in vehicle- and erythropoietin-treated animals (not shown), SPRR1A was abundant after ischaemia in the ipsilesional motor cortex (Fig. 8). In line with reduced SPRR1 messenger RNA levels, erythropoietin markedly diminished the expression of SPRR1 protein at Days 14 and 30 post-ischaemia (Fig. 8). Our data suggest that brain plasticity is actively inhibited by erythropoietin in the ischaemic hemisphere.
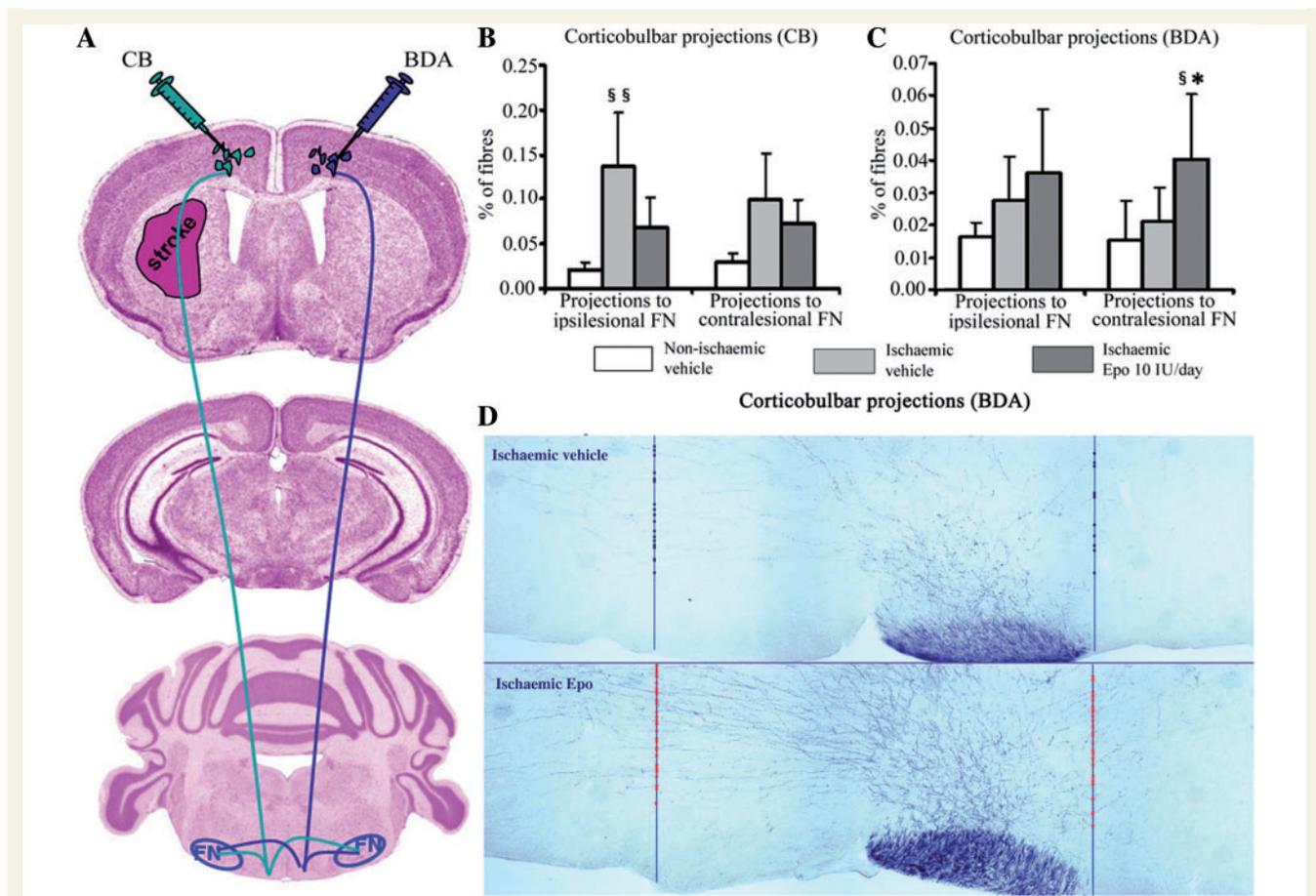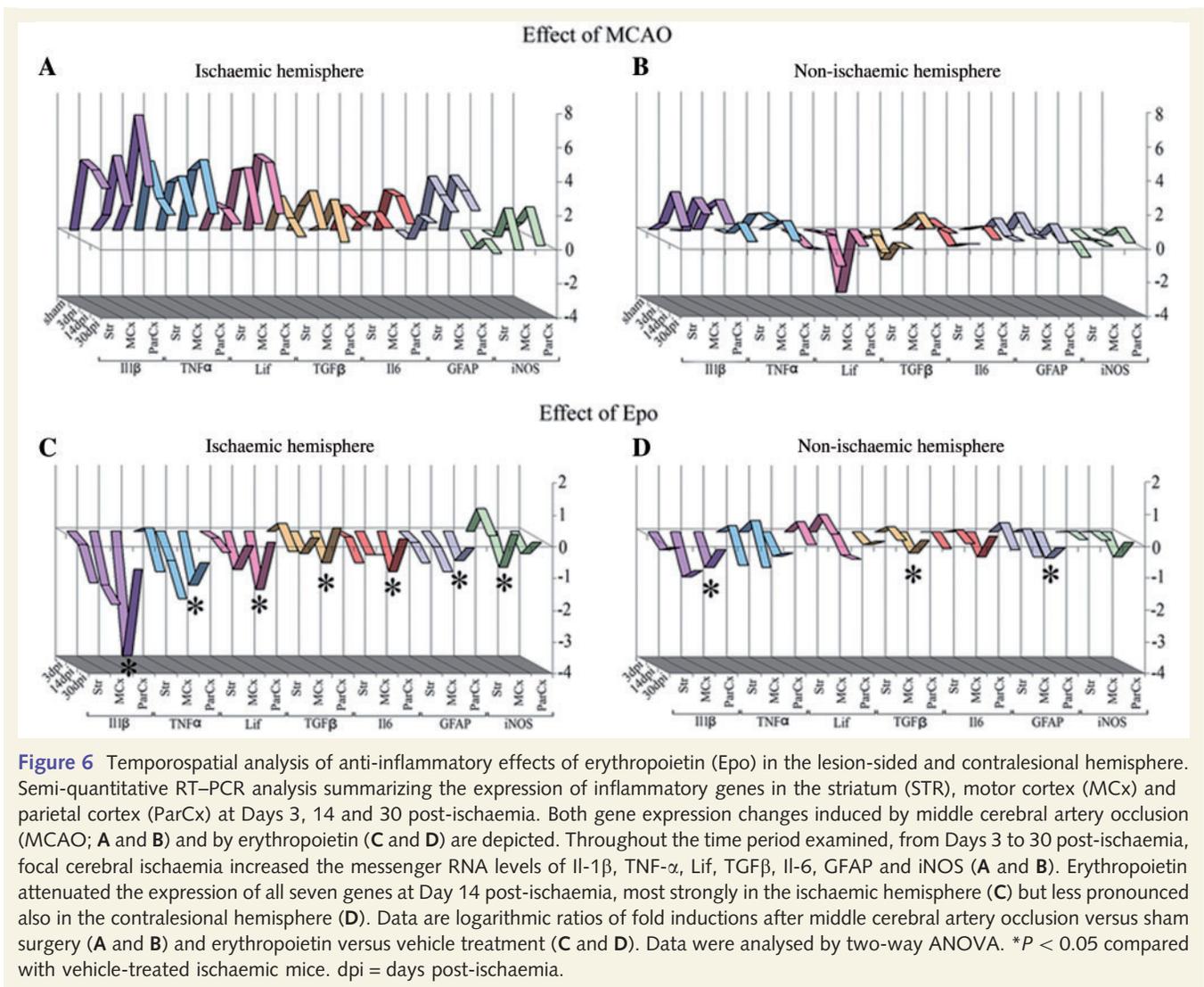
Figure 5 Erythropoietin (Epo) increases contralesional corticobulbar plasticity without influencing ipsilesional corticobulbar plasticity that is increased by the stroke. Tract tracing analysis of corticobulbar projections ipsilateral and contralateral to the stroke at the level of the facial nucleus (FN) in mice receiving cascade blue-labelled (CB) and BDA injections into the ipsilesional and contralesional motor cortex (placement of tracer injections shown in **A**). Percent of fibres leaving the pyramidal tract in direction of the ipsilesional and contralesional facial nucleus traced by (**B**) cascade blue and (**C**) BDA. Note that the percentage of fibres projecting to the ipsilesional facial nucleus after cascade blue injection into the lesion-sided motor cortex significantly increases in response to stroke (**B**). Interestingly, erythropoietin does not further strengthen this ipsilesional projection, but rather reduces it (**B**), simultaneously increasing the percentage of BDA stained contralesional pyramidal tract fibres innervating the contralesional facial nucleus (**C**). (**D**) Microphotographs of representative ischaemic vehicle- and erythropoietin-treated mice showing BDA-traced corticobulbar fibres crossing the intersection lines (superimposed in blue) on both sides of the brain. Note that erythropoietin increases fibre outgrowth towards the contralesional facial nucleus (intersecting fibres labelled with dots). Data are means ±SD. Data were analysed by one-way ANOVA followed by least significant differences tests. $^{§}P < 0.05/^{§§}P < 0.01$ compared with vehicle-treated non-ischaemic mice. $^{*}P < 0.05$ compared with vehicle-treated ischaemic mice.

Discussion

Using a comprehensive analysis of (i) motor and coordination deficits; (ii) reorganization processes of the peri-ischaemic tissue and (iii) pyramidal tract plasticity both ipsilateral and contralateral to the stroke, we have shown that post-acute delivery of recombinant human erythropoietin, initiated as late as 72 h after focal cerebral ischaemia, promotes functional neurological recovery in mice submitted to transient intraluminal middle cerebral artery occlusion by mechanisms involving perilesional tissue remodelling and promotion of contralateral pyramidal tract plasticity. We used an experimental delivery protocol, in which erythropoietin was administered into the lateral ventricle from Days 3–30 post-ischaemia via mini osmotic pumps. In addition

to tract-tracing studies, we performed a detailed analysis of histochemical and molecular biological changes induced by erythropoietin, showing that the growth factor inhibits inflammatory responses of the brain tissue and at the same time modulates plasticity genes.

That erythropoietin promotes neurological recovery beyond the acute stroke phase is noteworthy, and it opens new perspectives for post-acute therapies. In contrast to acute neuroprotection, which aims at preserving ischaemic neurons from apoptotic or necrotic injury and which in case of existing studies can hardly be expected beyond a time-window of 3–6 h after the stroke (Minnerup *et al.*, 2009), post-acute therapies aim at the reorganization of the brain, both in the vicinity (Cramer and Chopp, 2000) and areas remote (Wiessner *et al.*, 2003) to the stroke lesion.

Figure 6 Temporospatial analysis of anti-inflammatory effects of erythropoietin (Epo) in the lesion-sided and contralesional hemisphere. Semi-quantitative RT–PCR analysis summarizing the expression of inflammatory genes in the striatum (STR), motor cortex (MCx) and parietal cortex (ParCx) at Days 3, 14 and 30 post-ischaemia. Both gene expression changes induced by middle cerebral artery occlusion (MCAO; **A** and **B**) and by erythropoietin (**C** and **D**) are depicted. Throughout the time period examined, from Days 3 to 30 post-ischaemia, focal cerebral ischaemia increased the messenger RNA levels of Il-1β, TNF-α, Lif, TGFβ, Il-6, GFAP and iNOS (**A** and **B**). Erythropoietin attenuated the expression of all seven genes at Day 14 post-ischaemia, most strongly in the ischaemic hemisphere (**C**) but less pronounced also in the contralesional hemisphere (**D**). Data are logarithmic ratios of fold inductions after middle cerebral artery occlusion versus sham surgery (**A** and **B**) and erythropoietin versus vehicle treatment (**C** and **D**). Data were analysed by two-way ANOVA. *$P < 0.05$ compared with vehicle-treated ischaemic mice. dpi = days post-ischaemia.

Slowly progressive secondary degeneration takes place in the striatum of vehicle-treated mice submitted to transient intraluminal middle cerebral artery occlusion, reflected by a continued loss of neurons and secondary tissue shrinkage, both of which were reduced by erythropoietin in our study. Our observations are in line with a previous study (Bacigaluppi et al., 2009), which reported secondary degeneration of the ipsilesional striatum in ischaemic mice that was antagonized by adult neural precursor (i.e. stem) cells. Similar to the present study, this effect was not evident in the initial recovery phase, but developed within 2–4 weeks after the stroke. Inhibition of caspase-3-dependent apoptotic cell injury was noticed in the striatum in that study (Bacigaluppi et al., 2009), indicating that the prevention of shrinkage represented a delayed neuroprotective effect. That secondary neurodegeneration in the vicinity of the lesion may be relevant for stroke recovery has also been proposed by Taguchi et al. (2007), who reported that administration of granulocyte colony-stimulating factor after stroke enhances inflammatory response both ipsi- and contralateral to the ischaemic side, correlating with a remarkable brain atrophy and an impaired functional

recovery after stroke. In the same study, erythropoietin treatment after stroke was proved to have beneficial effects by reducing brain atrophy and accelerating functional recovery after stroke. This reverse effect of erythropoietin is confirmed in the current study, in which we show that erythropoietin therapy reduces inflammatory response both ipsi- and contralateral to the ischaemic side, thereby reducing brain atrophy and increasing functional recovery after stroke.

Besides preventing delayed neurodegeneration, erythropoietin-induced angiogenesis and inhibited reactive astrogliosis, at the same time preventing scar formation of ischaemic tissue. Our data are in agreement with recent studies by Li et al. (2009), who observed, with MRI, peri-lesional white matter remodelling in middle cerebral artery occlusion rats treated with erythropoietin within 24 h of reperfusion. Inhibition of glial scar formation has previously been reported in studies evaluating cell-based therapies, namely bone marrow-derived stem cells (Li et al., 2005) and adult neural precursor cells (Bacigaluppi et al., 2009), indicating that erythropoietin shares common mechanisms of action with these cells. In contrast to erythropoietin, adult neural stem/precursor

Figure 7 Temporospatial analysis of plasticity-promoting and -inhibitory effects of erythropoietin (Epo) in the lesion-sided and contralesional hemisphere. Semi-quantitative RT–PCR analysis summarizing the expression of pro-plasticity and anti-plasticity genes that were regulated by the stroke in the striatum (STR), motor cortex (MCx) and parietal cortex (ParCx) at Days 3, 14 and 30 post-ischaemia. Both gene expression changes induced by middle cerebral artery occlusion (MCAO; **A** and **B**) and by erythropoietin (**C** and **D**) are summarized. Throughout the time period examined, focal cerebral ischaemia elevated the messenger RNA levels of different pro-plasticity genes, namely of SPRR1 and IGF-1, in the ischaemic hemisphere (**A**). Interestingly, erythropoietin reduced the expression of SPRR1, IGF-1, BDNF and KDR at Day 14 post-ischaemia in the ischaemic hemisphere (**A**), at the same time downregulating the anti-plasticity genes neurocan and ephrin-B1 more clearly contralateral (**B**) that ipsilateral (**A**) to the stroke. Data are logarithmic ratios of fold inductions after middle cerebral artery occlusion versus sham surgery (**A** and **B**) and erythropoietin versus vehicle treatment (**C** and **D**). Data were analysed by two-way ANOVA. *$P < 0.05$ compared with vehicle-treated ischaemic mice. dpi = days post-ischaemia.

cells did not stimulate angiogenesis (Bacigaluppi et al., 2009). An advantage of erythropoietin as compared to cell-based therapies, namely with neural precursor cells, is the lack of malignant tumour growth, which still remains a risk for the latter cells that cannot entirely be ruled out (Amariglio et al., 2009).

In our study, induction of focal cerebral ischaemia significantly increased axonal plasticity ipsilateral to the stroke, namely at the level of the facial nucleus. Pyramidal tract remodelling was recently examined by means of manganese-enhanced MRI in rats from 4 to 10 weeks after 90 min middle cerebral artery occlusion (van der Zijden et al., 2008). In that study, significantly increased manganese transport was observed in lesion-contralateral brain structures after ipsilesional motor cortex injections, suggesting enhanced interhemispheric axonal growth (van der Zijden et al., 2008). Unlike dextran amines, manganese is a combined anterograde (Canals et al., 2008) and retrograde (Matsuda et al., 2010) tracer, which is also trans-synaptically transported. Manganese therefore does not provide more detailed insights into plasticity processes. It has previously been shown, however, by means of

histochemistry, that focal cerebral ischaemia induces the growth of short distance fibres (Carmichael et al., 2001) and promotes dendritic spine formation (Brown et al., 2007) in the perilesional tissue ipsilateral to the stroke. Our data confirm that plasticity is induced and that it not only affects short distance but also long distance projections.

In view of the enhanced plasticity ipsilateral to the stroke, which we observed in vehicle-treated ischaemic mice, it is noteworthy that erythropoietin did not further enhance ipsilesional pyramidal tract plasticity but rather reduced it ($P = 0.07$ at the level of the facial nucleus). Instead, erythropoietin significantly increased the projections from the contralesional motor cortex towards the denervated red and facial nuclei. Contralesional sprouting was shown to correlate with functional neurological recovery after antagonization of the neurite growth inhibitor NogoA (Papadopoulos et al., 2002; Wiessner et al., 2003) and bone marrow-derived stem cell therapy (Andrews et al., 2008). In case of neutralizing NogoA antibodies, close correlations between the degree of functional neurological recovery and contralateral sprouting have been reported
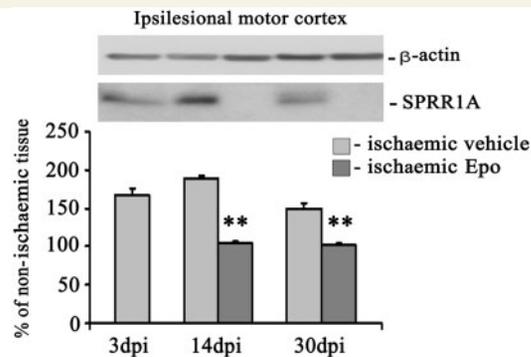
Figure 8 Erythropoietin (Epo) downregulates SPRR1A protein in the lesion-sided motor cortex. Western blot analysis showing reduced abundance of SPRR1A in erythropoietin- as compared with vehicle-treated mice at Days 14 and 30 post-ischaemia. Protein loading was controlled by reprobing the blots with a β-actin antibody. SPRR1A levels were densitometrically analysed. Data are mean values ±SD. Data were evaluated by two-way ANOVA followed by two-tailed t-tests for both time points. $**P < 0.01$ compared with vehicle-treated ischaemic mice.

(Papadopoulos *et al.*, 2002; Wiessner *et al.*, 2003), demonstrating that cerebral connectivity represents a useful marker of recovery processes. Our data confirm that stroke induces plasticity in the lesioned hemisphere and that erythropoietin shifts plasticity towards the contralesional hemisphere with a beneficial effect on functional recovery.

In this study, erythropoietin exhibited pronounced anti-inflammatory actions, which went along with a reduction of leucocyte infiltration that persisted as long as erythropoietin was infused. It has already been shown that erythropoietin and its non-erythropoietic derivatives exhibit anti-inflammatory actions when delivered in the acute stroke phase. As such, reduced leucocyte infiltration (Villa *et al.*, 2003, 2007), decreased release of TNF-α, IL-6 and monocyte chemoattractant protein-1 (Villa *et al.*, 2003) and diminished expression of inducible nitric oxide synthase (Kilic *et al.*, 2005*a*) were noticed. In cell culture, astrocytes but not leucocytes were shown to be responsive to erythropoietin administration (Villa *et al.*, 2003), suggesting that reduced release of inflammatory signals may be the trigger for the reduced invasion of blood-borne cells into the brain. By means of RT–PCR, we revealed that erythropoietin downregulated several pro-inflammatory genes IL-1β, TNF-α, LIF, TGF-β, IL-6, glial fibrillary acidic protein and inducible nitric oxide synthase, indicating that anti-inflammation may represent a mode of action, via which this growth factor enables brain reorganization. Interestingly, pump removal in our study resulted in a rebound of leucocyte infiltration in erythropoietin-treated mice, which did not, however, result in the re-emergence of neurological deficits. Our data argue in favour of a critical time window in which inflammatory responses deteriorate recovery processes in the ischaemic brain.

Further to this, RT–PCR-based profiling of pro-plasticity genes showed that erythropoietin diminished the expression of pro-plasticity messenger RNAs SPRR1, IGF-1 and KDR in the ischaemic

hemisphere that were increased by the stroke. At the same time, erythropoietin downregulated the anti-plasticity messenger RNAs neurocan and ephrin B1 and upregulated the pro-plasticity SPRR1 in the non-ischaemic hemisphere. In case of SPRR1A, downregulation was also demonstrated on the protein level by means of western blots. Upregulation of pro-plasticity markers in the lesion border zone has previously been described after permanent cortical ischaemia for SPRR1, MARCKS, growth-associated protein 43 and synaptophysin, as well as delayed upregulation of anti-plasticity markers for neurocan and ephrin B1 (Stroemer *et al.*, 1995; Carmichael and Li, 2006). In our study, erythropoietin regulated several pro- and anti-plasticity genes especially in the non-ischaemic hemisphere at Day 30 post-stroke, thus providing evidence for a specific plasticity modulating action of this growth factor. This is in accordance to previous studies on plasticity-promoting actions of erythropoietin in rodent models of Parkinson's disease (McLeod *et al.*, 2006) and following optic nerve transection (King *et al.*, 2007). We have shown that erythropoietin's plasticity effects are relevant for stroke recovery processes.

After the German multicentre erythropoietin trial, which has recently shown unfavourable effects of erythropoietin in patients undergoing thrombolysis (Ehrenreich *et al.*, 2009), presumably via exacerbation of extracellular matrix degradation by combined tissue-plasminogen activator/erythropoietin treatment (Zechariah *et al.*, 2010), further neuroprotection studies with erythropoietin in the acute stroke phase are unlikely. Our present study offers a basis for the prolongation of timeframes far into the sub-acute stroke phase, thus paving the way for plasticity-promoting trials with erythropoietin, its non-erythropoietic derivatives (Leist *et al.*, 2004) or with small molecule agonists of erythropoietin receptors (Pankratova *et al.*, 2010). The latter compounds, for which the utility for systemic delivery still has to be shown, may specifically be tailored to bind to erythropoietin's CNS receptors. Non-erythropoietic derivatives of erythropoietin do not induce haemoglobin or coagulation changes, and thus do not bear an elevated risk of thromboembolic events, which has recently been discussed in the context of chronic kidney disease trials (Pfeffer *et al.*, 2009). With these considerations, proof-of-concept studies in human patients are promising.

Supplementary material

Supplementary material is available at *Brain* online.

References

Amariglio N, Hirshberg A, Scheithauer BW, Cohen Y, Loewenthal R, Trakhtenbrot L, et al. Donor-derived brain tumor following neural stem cell transplantation in an ataxia telangiectasia patient. Plos Med 2009; 6: e1000029.

Andrews EM, Tsai SY, Johnson SC, Farrer JR, Wagner JP, Kopen GC, et al. Human adult bone marrow-derived somatic cell therapy results in functional recovery and axonal plasticity following stroke in the rat. Exp Neurol 2008; 211: 588–92.

Bacigaluppi M, Pluchino S, Jametti LP, Kilic E, Kilic Ü, Salani G, et al. Delayed post-ischemic neuroprotection following systemic neural stem cell transplantation involves multiple mechanisms. Brain 2009; 132: 2239–51.

Bernaudin M, Bellail A, Marti HH, Yvon A, Vivien D, Duchatelle I, et al. Neurons and astrocytes express EPO mRNA: oxygen-sensing mechanisms that involve the redox-state of the brain. Glia 2000; 30: 271–8.

Bernaudin M, Marti HH, Roussel S, Divoux D, Nouvelot A, MacKenzie ET, et al. A potential role for erythropoietin in focal permanent cerebral ischemia in mice. J Cereb Blood Flow Metab 1999; 19: 643–51.

Biernaskie J, Chernenko G, Corbett D. Efficacy of rehabilitative experience declines with time after focal ischemic brain injury. J Neurosci 2004; 24: 1245–54.

Bonita R, Anderson CS, Broad JB, Jamrozik KD, Stewart-Wynne EG, Anderson NE. Stroke incidence and case fatality in Australasia. A comparison of the Auckland and Perth population-based stroke registers. Stroke 1994; 25: 552–7.

Brown CE, Li P, Boyd JD, Delaney KR, Murphy TH. Extensive turnover of dendritic spines and vascular remodeling in cortical tissues recovering from stroke. J Neurosci 2007; 27: 4101–9.

Buchli AD, Schwab ME. Inhibition of Nogo: a key strategy to increase regeneration, plasticity and functional recovery of the lesioned central nervous system. Ann Med 2005; 37: 556–67.

Canals S, Beyerlein M, Keller AL, Murayama Y, Logothetis NK. Magnetic resonance imaging of cortical connectivity in vivo. Neuroimage 2008; 40: 458–72.

Carmichael ST, Li S. Growth-associated gene and protein expression in the region of axonal sprouting in the aged brain after stroke. Neurobiol Dis 2006; 23: 362–73.

Carmichael ST, Wei L, Rovainen CM, Woolsey TA. New patterns of intracortical projections after focal cortical stroke. Neurobiol Dis 2001; 8: 910–22.

Chen J, Zhang ZG, Li Y, Wang Y, Wang L, Zhang C, et al. Statins induce angiogenesis, neurogenesis, and synaptogenesis after stroke. Ann Neurol 2003; 53: 743–51.

Cramer SC, Chopp M. Recovery recapitulates ontogeny. Trends Neurosci 2000; 23: 265–71.

Cramer SC, Nelles G, Benson RR, Kaplan JD, Parker RA, Kwong KK, et al. A functional MRI study of subjects recovered from hemiparetic stroke. Stroke 1997; 28: 2518–27.

Ding G, Jiang Q, Li L, Zhang L, Zhang ZG, Ledbetter KA, et al. Magnetic resonance imaging investigation of axonal remodeling and angiogenesis after embolic stroke in sildenafil-treated rats. J Cereb Blood Flow Metab 2008; 28: 1440–8.

Dobkin BH. Neurologic rehabilitation. Philadelphia: FA Davis; 1996.

Ehrenreich H, Hasselblatt M, Dembowski C, Cepek L, Lewczuk P, Stiefel M, et al. Erythropoietin therapy for acute stroke is both safe and beneficial. Mol Med 2002; 8: 495–505.

Ehrenreich H, Weissenborn K, Prange H, Schneider D, Weimar C, Wartenberg K, et al. Recombinant human erythropoietin in the treatment of acute ischemic stroke. Stroke 2009; 40: e647–56.

Gerloff C, Bushara K, Sailer A, Wassermann EM, Chen R, Matsuoka T, et al. Multimodal imaging of brain reorganization in motor areas of the contralesional hemisphere of well recovered patients after capsular stroke. Brain 2006; 129: 791–808.

Grimm C, Hermann DM, Bogdanova A, Hotop S, Kilic U, Wenzel A, et al. Neuroprotection by hypoxic preconditioning: HIF-1 and erythropoietin protect from retinal degeneration. Semin Cell Dev Biol 2005; 16: 531–8.

Hacke W, Kaste M, Bluhmki E, Brozman M, Davalos A, Guidetti D, et al. Thrombolysis with alteplase 3 to 4.5 hours after acute ischemic stroke. N Engl J Med 2008; 359: 1317–29.

Hermann DM, Zechariah A. Implications of vascular endothelial growth factor for postischemic neurovascular remodeling. J Cereb Blood Flow Metab 2009; 29: 1620–43.

Hudson JQ, Sameri RM. Darbepoetin alfa, a new therapy for the management of anemia of chronic kidney disease. Pharmacotherapy 2002; 22: 141S–9S.

Kilic E, ElAli A, Kilic Ü, Guo Z, Ugur M, Uslu U, et al. Role of Nogo-A in neuronal survival in the reperfused ischemic brain. J Cereb Blood Flow Metab 2010; 30: 969–84.

Kilic E, Kilic Ü, Soliz J, Bassetti CL, Gassmann M, Hermann DM. Brain-derived erythropoietin protects from focal cerebral ischemia by dual activation of ERK-1/-2 and Akt pathways. FASEB J 2005a; 19: 2026–8.

Kilic Ü, Kilic E, Soliz J, Bassetti CL, Gassmann M, Hermann DM. Erythropoietin protects from axotomy-induced degeneration of retinal ganglion cells by activating ERK-1/-2. FASEB J 2005b; 19: 249–51.

Kilic E, Kilic Ü, Wang Y, Bassetti CL, Marti HH, Hermann DM. The phosphatidylinositol-3 kinase/Akt pathway mediates VEGF's neuroprotective activity and induces blood brain barrier permeability after focal cerebral ischemia. FASEB J 2006; 20: 1185–7.

Kilic E, Spudich A, Kilic Ü, Rentsch KM, Vig R, Matter CM, et al. ABCC1: a gateway for pharmacological compounds to the ischaemic brain. Brain 2008; 131: 2679–89.

King CE, Rodger J, Bartlett C, Esmaili T, Dunlop SA, Beazley LD. Erythropoietin is both neuroprotective and neuroregenerative following optic nerve transection. Exp Neurol 2007; 205: 48–55.

Leist M, Ghezzi P, Grasso G, Bianchi R, Villa P, et al. Fratelli M Derivatives of erythropoietin that are tissue protective but not erythropoietic. Science 2004; 305: 239–42.

Li Y, Chen J, Zhang CL, Wang L, Lu D, Katakowski M, et al. Gliosis and brain remodeling after treatment of stroke in rats with marrow stromal cells. Glia 2005; 49: 407–17.

Li L, Jiang Q, Ding G, Zhang L, Zhang ZG, Li Q, et al. MRI identification of white matter reorganisation enhanced by erythropoietin treatment in a rat model of focal ischemia. Stroke 2009; 40: 936–41.

Li Y, Lu Z, Keogh CL, Yu SP, Wei L. Erythropoietin-induced neurovascular protection, angiogenesis, and cerebral blood flow restoration after focal cerebral ischemia in mice. J Cereb Blood Flow Metab 2007; 27: 1043–54.

Marti HH, Wenger RH, Rivas LA, Straumann U, Digicaylioglu M, Henn V, et al. Erythropoietin gene expression in human, monkey and murine brain. Eur J Neurosci 1996; 8: 666–76.

Matsuda K, Wang HX, Suo C, McCombe D, Horne MK, Morrison WA, et al. Retrograde axonal tracing using manganese enhanced magnetic resonance imaging. Neuroimage 2010; 50: 366–74.

McLeod M, Hong M, Mukhida K, Sadi D, Ulalia R, Mendez I. Erythropoietin and GDNF enhance ventral mesencephalic fiber outgrowth and capillary proliferation following neural transplantation in a rodent model of Parkinson's disease. Eur J Neurosci 2006; 24: 361–70.

Minnerup J, Heidrich J, Rogalewski A, Schäbitz W-R, Wellmann J. The efficacy of erythropoietin and its analogues in animal stroke models: a meta-analysis. Stroke 2009; 40: 3113–20.

Musso M, Weiller C, Kiebel S, Müller S, Bülau P, Rijntjes M. Training-induced brain plasticity in aphasia. Brain 1999; 122: 1782–90.

Pankratova S, Kiryushko D, Sonn K, Soroka V, Køhler LB, Rathje M, et al. Neuroprotective properties of a novel, non-haematopoietic agonist of the erythropoietin receptor. Brain 2010; 133: 2281–94.

Papadopoulos CM, Tsai S-Y, Alsbiei T, O'Brien TE, Schwab ME, Kartje GL. Functional recovery and neuroanatomical plasticity following middle cerebral artery occlusion and IN-1 antibody treatment in the adult rat. Ann Neurol 2002; 51: 433–41.

Pfeffer MA, Burdmann EA, Chen CY, Cooper ME, de Zeeuw D, Eckardt KU, et al. A trial of darbepoetin alfa in type 2 diabetes and chronic kidney disease. N Engl J Med 2009; 21: 2019–32.

Pluchino S, Muzio L, Imitola J, Deleidi M, Alfaro-Cervello C, Salani G, et al. Persistent inflammation alters the function of the endogenous brain stem cell compartment. Brain 2008; 131: 2564–78.

Seymour AB, Andrews EM, Tsai S-Y, Markus TM, Bollnow MR, Brenneman MM, et al. Delayed treatment with monoclonal antibody IN-1 1 week after stroke results in recovery of function and corticorubral plasticity in adult rats. J Cereb Blood Flow Metab 2005; 25: 1366–75.

Siren AL, Fratelli M, Brines M, Goemans C, Casagrande S, Lewczuk P, et al. Erythropoietin prevents neuronal apoptosis after cerebral ischemia and metabolic stress. Proc Natl Acad Sci USA 2001; 98: 4044–9.

Stroemer RP, Kent TA, Hulsebosch CE. Neocortical neuronal sprouting, synaptogenesis, and behavioral recovery after neocortical infarction in rats. Stroke 1995; 26: 2135–44.

Tan CC, Eckardt KU, Firth JD, Ratcliffe PJ. Feedback modulation of renal and hepatic erythropoietin mRNA in response to graded anemia and hypoxia. Am J Physiol 1992; 263: F474–81.

Taguchi A, Wen Z, Myojin K, Yoshihara T, Nakagomi T, Nakayama D, et al. Granulocyte colony-stimulating factor has a negative effect on stroke outcome in a murine model. Eur J Neurosci 2007; 26: 126–33.

van der Zijden JP, Bouts MJ, Wu O, Roeling TAP, Bleys RL, van der Toorn A, et al. Manganese-enhanced MRI of brain plasticity in relation to functional recovery after experimental stroke. J Cereb Blood Flow Metab 2008; 28: 832–40.

Villa P, Bigini P, Mennini T, Agnello D, Laragione T, Cagnotto A, et al. Erythropoietin selectively attenuates cytokine production and inflammation in cerebral ischemia by targeting neuronal apoptosis. J Exp Med 2003; 198: 971–5.

Villa P, van Beek J, Larsen AK, Gerwien J, Christensen S, Cerami A, et al. Reduced functional deficits, neuroinflammation, and secondary tissue damage after treatment of stroke by nonerythropoietic erythropoietin derivates. J Cereb Blood Flow Metab 2007; 27: 552–63.

Wang L, Zhang Z, Wang Z, Zhang R, Chopp M. Treatment of stroke with erythropoietin enhances neurogenesis and angiogenesis and improves neurological function in rats. Stroke 2004; 35: 1732–7.

Wiessner C, Bareyre FM, Allegrini PR, Mir AK, Frentzel S, Zurini M, et al. Anti-Nogo-A antibody infusion 24 hours after experimental stroke improved behavioral outcome and corticospinal plasticity in normotensive and spontaneously hypertensive rats. J Cereb Blood Flow Metab 2003; 23: 154–65.

Zechariah A, ElAli A, Hermann DM. Combination of tissue-plasminogen activator with erythropoietin induces blood-brain barrier permeability, extracellular matrix degeneration and DNA fragmentation after focal cerebral ischemia in mice. Stroke 2010; 41: 1008–12.

Z'Graggen WJ, Metz GA, Kartje GL, Thallmair M, Schwab ME. Functional recovery and enhanced corticofugal plasticity after unilateral pyramidal tract lesion and blockade of myelin-associated neurite growth inhibitors in adult rats. J Neurosci 1998; 18: 4744–57.